Supporting Information for "Observed Seasonal Evolution of the Antarctic Slope Current System at the Coast of Dronning Maud Land, East Antarctica"

Julius Lauber[1,2], Laura de Steur[1], Tore Hattermann[1], Elin Darelius[2,3]

[1]Norwegian Polar Institute, Tromsø, Norway

[2]Geophysical Institute, University of Bergen, Bergen, Norway

[3]Bjerknes Centre for Climate Research, Bergen, Norway

Contents of this file

1. Text S1
2. Figures S1 to S4
3. Tables S1 to S2

Introduction This file contains one text and several figures and tables that supplement the analyses presented in the main text: Text S1 describes how uncertainties of the velocity estimates were calculated. Fig. S1 shows time series of oxygen in comparison with salinity. Fig. S2 shows the seasonal time-depth evolution of salinity at the mooring bathymetries for the H18 data. Fig. S3 shows the seasonal thermocline depth evolution in time-bathymetry space for the H18 data. Fig. S4 shows the $DML_{shallow}$ and $DML_{shallow}$

Corresponding author: J. Lauber, Norwegian Polar Institute, Hjalmar Johansens gate 14, 9296 Tromsø, Norway. (julius.lauber@npolar.no)

temperature time series in comparison to the climatological temperature from moorings AWI233 and AWI232 at the prime meridian. Tables S1 and S2 show details of all instruments at $\mathrm{DML_{shallow}}$ and $\mathrm{DML_{deep}}$, respectively.

Text S1: Uncertainties of velocity estimates

The uncertainty of the satellite-derived surface geostrophic velocity climatology (Fig. 6a) is obtained by taking the standard deviation at the respective data point and for all available data during respective month from April 2013 to July 2019.

The uncertainty of UBT_{obs} (Fig. 6b, Eqn. 2 in the main text) is estimated as follows: First, the error of the velocity measured by the two 150 kHz ADCPs at depth is obtained as given by the manufacturer (Teledyne Marine, 2023):

$$\sigma_{U_{ADCP}} = 0.005\, U_{ADCP} + 0.5\,\mathrm{cm\,s^{-1}} \tag{1}$$

Here, U_{ADCP} is the velocity measured by the ADCPs. This error is propagated to UBT_{obs}, which is the average of the lowermost 12 ADCP bins at depth, according to Gauss' law of error propagation:

$$\sigma_{UBT_{obs_{prelim}}} = \frac{1}{N}\sqrt{\sum_{i=1}^{N} \sigma^2_{U_{ADCP_i}}} \tag{2}$$

Here, $N = 12$ is the number of bins over which the average is taken. To also take into account the fact that the vertical gradient in velocity is not exactly zero at the ADCP depths, as seen in Fig. 5, the standard deviation over the 12 bins, $\sigma_{U_{ADCP_{\Delta z}}}$, is added to $\sigma_{UBT_{obs_{prelim}}}$, so that the final uncertainty of UBT_{obs} is

$$\sigma_{UBT_{obs}} = \frac{1}{N}\sqrt{\sum_{i=1}^{N}\sigma^2_{U_{ADCP_i}}} + \sigma_{U_{ADCP_{\Delta z}}}. \tag{3}$$

The uncertainty of UBC_{obs} (Fig. 6d, Eqn. 4 in the main text), calculated as the difference between the observed velocity at the uppermost bin of the near-surface ADCPs (U_{ADCP}) and UBT_{obs}, is estimated as follows: During times when measurements at this bin are available, the uncertainty of U_{ADCP} is calculated according to Eqn. 1. When no measurements are available, mostly during the winter months due to reduced primary production and resulting reduced backscatter, the uncertainty of the extrapolated value is obtained from the uncertainty of the vertical linear regression according to

$$\sigma_{U_{ADCP}} = \sqrt{\sigma_a^2 + d^2\sigma_b^2}. \tag{4}$$

Here, σ_a and σ_b are the uncertainties of the axis intercept and slope of the linear regression, respectively, and d is the depth of the uppermost ADCP bin, i.e. 100 m at $\mathrm{DML_{shallow}}$ and 20 m at $\mathrm{DML_{deep}}$. The error propagation from the uncertainty of the linear regression is sufficient to estimate the uncertainty of the extrapolated value since, tested during periods when all bins were available, the extrapolation generally did not lead to an overestimate of the velocity at the depth of the uppermost bin. Again from error propagation, the final uncertainty of UBC_{obs} is then

$$\sigma_{UBC_{obs}} = \sqrt{\sigma^2_{U_{ADCP}} + \sigma^2_{UBT_{obs}}}. \tag{5}$$

We refrain from estimating uncertainties for UBC_{H18} since the H18 data are based on over 40 years of data across different observational platforms. Since UBT_{H18A22} is derived from UBC_{H18}, we also do not provide uncertainty for this velocity estimate.

References

Fahrbach, E., & Rohardt, G. (2012a). Physical oceanography and current meter data from mooring AWI232-1. *Alfred Wegener Institute, Helmholtz Centre for Polar and Marine Research, Bremerhaven, PANGAEA.* (URL: https://doi.org/10.1594/PANGAEA.793090. Last accessed: 11.06.2022)

Fahrbach, E., & Rohardt, G. (2012b). Physical oceanography and current meter data from mooring AWI232-2. *Alfred Wegener Institute, Helmholtz Centre for Polar and Marine Research, Bremerhaven, PANGAEA.* (URL: https://doi.org/10.1594/PANGAEA.793091. Last accessed: 11.06.2022)

Fahrbach, E., & Rohardt, G. (2012c). Physical oceanography and current meter data from mooring AWI232-3. *Alfred Wegener Institute, Helmholtz Centre for Polar and Marine Research, Bremerhaven, PANGAEA.* (URL: https://doi.org/10.1594/PANGAEA.793092. Last accessed: 11.06.2022)

Fahrbach, E., & Rohardt, G. (2012d). Physical oceanography and current meter data from mooring AWI232-4. *Alfred Wegener Institute, Helmholtz Centre for Polar and Marine Research, Bremerhaven, PANGAEA.* (URL: https://doi.org/10.1594/PANGAEA.793093. Last accessed: 11.06.2022)

Fahrbach, E., & Rohardt, G. (2012e). Physical oceanography and current meter data from mooring AWI232-5. *Alfred Wegener Institute, Helmholtz Centre for Polar and Marine Research, Bremerhaven, PANGAEA.* (URL: https://doi.org/10.1594/

PANGAEA.793094. Last accessed: 11.06.2022)

Fahrbach, E., & Rohardt, G. (2012f). Physical oceanography and current meter data from mooring AWI232-6. *Alfred Wegener Institute, Helmholtz Centre for Polar and Marine Research, Bremerhaven, PANGAEA*. (URL: https://doi.org/10.1594/PANGAEA.793095. Last accessed: 11.06.2022)

Fahrbach, E., & Rohardt, G. (2012g). Physical oceanography and current meter data from mooring AWI233-1. *Alfred Wegener Institute, Helmholtz Centre for Polar and Marine Research, Bremerhaven, PANGAEA*. (URL: https://doi.org/10.1594/PANGAEA.793096. Last accessed: 11.06.2022)

Fahrbach, E., & Rohardt, G. (2012h). Physical oceanography and current meter data from mooring AWI233-2. *Alfred Wegener Institute, Helmholtz Centre for Polar and Marine Research, Bremerhaven, PANGAEA*. (URL: https://doi.org/10.1594/PANGAEA.793097. Last accessed: 11.06.2022)

Fahrbach, E., & Rohardt, G. (2012i). Physical oceanography and current meter data from mooring AWI233-3. *Alfred Wegener Institute, Helmholtz Centre for Polar and Marine Research, Bremerhaven, PANGAEA*. (URL: https://doi.org/10.1594/PANGAEA.793098. Last accessed: 11.06.2022)

Fahrbach, E., & Rohardt, G. (2012j). Physical oceanography and current meter data from mooring AWI233-4. *Alfred Wegener Institute, Helmholtz Centre for Polar and Marine Research, Bremerhaven, PANGAEA*. (URL: https://doi.org/10.1594/PANGAEA.793099. Last accessed: 11.06.2022)

Fahrbach, E., & Rohardt, G. (2012k). Physical oceanography and current meter data from mooring AWI233-5. *Alfred Wegener Institute, Helmholtz Centre for Polar and*

Marine Research, Bremerhaven, PANGAEA. (URL: https://doi.org/10.1594/PANGAEA.793100. Last accessed: 11.06.2022)

Fahrbach, E., & Rohardt, G. (2012l). Physical oceanography and current meter data from mooring AWI233-6. *Alfred Wegener Institute, Helmholtz Centre for Polar and Marine Research, Bremerhaven, PANGAEA*. (URL: https://doi.org/10.1594/PANGAEA.793101. Last accessed: 11.06.2022)

Fahrbach, E., & Rohardt, G. (2012m). Physical oceanography and current meter data from mooring AWI233-7a. *Alfred Wegener Institute, Helmholtz Centre for Polar and Marine Research, Bremerhaven, PANGAEA*. (URL: https://doi.org/10.1594/PANGAEA.793102. Last accessed: 11.06.2022)

Fahrbach, E., & Rohardt, G. (2012n). Physical oceanography and current meter data from mooring AWI233-7b. *Alfred Wegener Institute, Helmholtz Centre for Polar and Marine Research, Bremerhaven, PANGAEA*. (URL: https://doi.org/10.1594/PANGAEA.793103. Last accessed: 11.06.2022)

Fahrbach, E., & Rohardt, G. (2013a). Physical oceanography and current meter data from mooring AWI232-7. *Alfred Wegener Institute, Helmholtz Centre for Polar and Marine Research, Bremerhaven, PANGAEA*. (URL: https://doi.org/10.1594/PANGAEA.818634. Last accessed: 11.06.2022)

Fahrbach, E., & Rohardt, G. (2013b). Physical oceanography and current meter data from mooring AWI232-8. *Alfred Wegener Institute, Helmholtz Centre for Polar and Marine Research, Bremerhaven, PANGAEA*. (URL: https://doi.org/10.1594/PANGAEA.818635. Last accessed: 11.06.2022)

Fahrbach, E., & Rohardt, G. (2013c). Physical oceanography and current meter data

from mooring AWI232-9. *Alfred Wegener Institute, Helmholtz Centre for Polar and Marine Research, Bremerhaven, PANGAEA*. (URL: https://doi.org/10.1594/PANGAEA.818636. Last accessed: 11.06.2022)

Rohardt, G., & Boebel, O. (2015). Physical oceanography and current meter data from mooring AWI232-11. *Alfred Wegener Institute, Helmholtz Centre for Polar and Marine Research, Bremerhaven, PANGAEA*. (URL: https://doi.org/10.1594/PANGAEA.846341. Last accessed: 11.06.2022)

Rohardt, G., & Boebel, O. (2017a). Physical oceanography and current meter data from mooring AWI232-10. *Alfred Wegener Institute, Helmholtz Centre for Polar and Marine Research, Bremerhaven, PANGAEA*. (URL: https://doi.org/10.1594/PANGAEA.875134. Last accessed: 11.06.2022)

Rohardt, G., & Boebel, O. (2017b). Physical oceanography and current meter data from mooring AWI232-12. *Alfred Wegener Institute, Helmholtz Centre for Polar and Marine Research, Bremerhaven, PANGAEA*. (URL: https://doi.org/10.1594/PANGAEA.875135. Last accessed: 11.06.2022)

Teledyne Marine. (2023). Workhorse II Data Sheet. *Teledyne RD Instruments*.

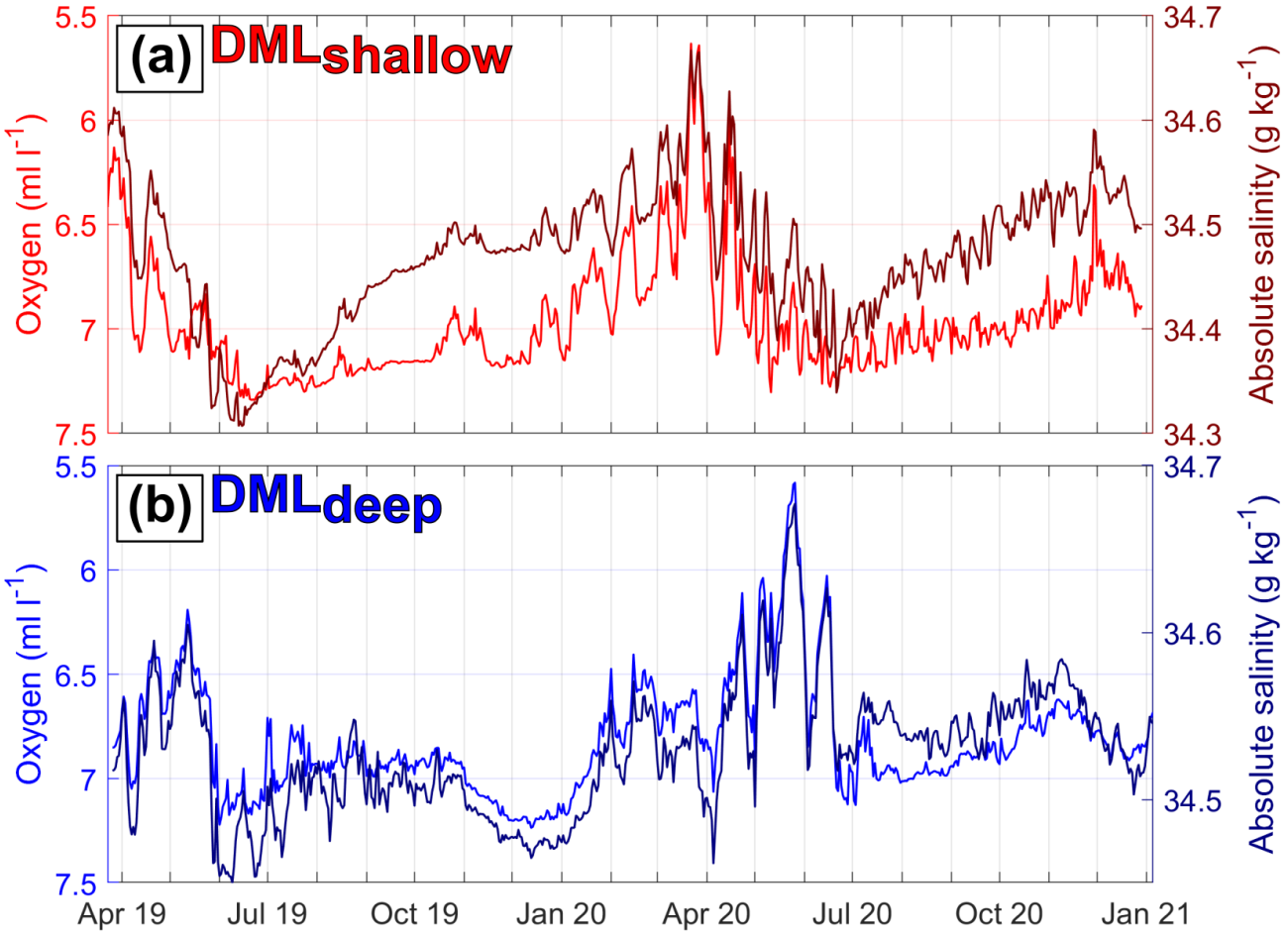

Figure S1. Daily averaged time series of oxygen (left axis) and absolute salinity (right axis) at the uppermost MicroCAT at (a) $DML_{shallow}$ (210 m) and (b) DML_{deep} (130 m). Note that the y-axis for oxygen has been reversed for better comparability with the salinity.

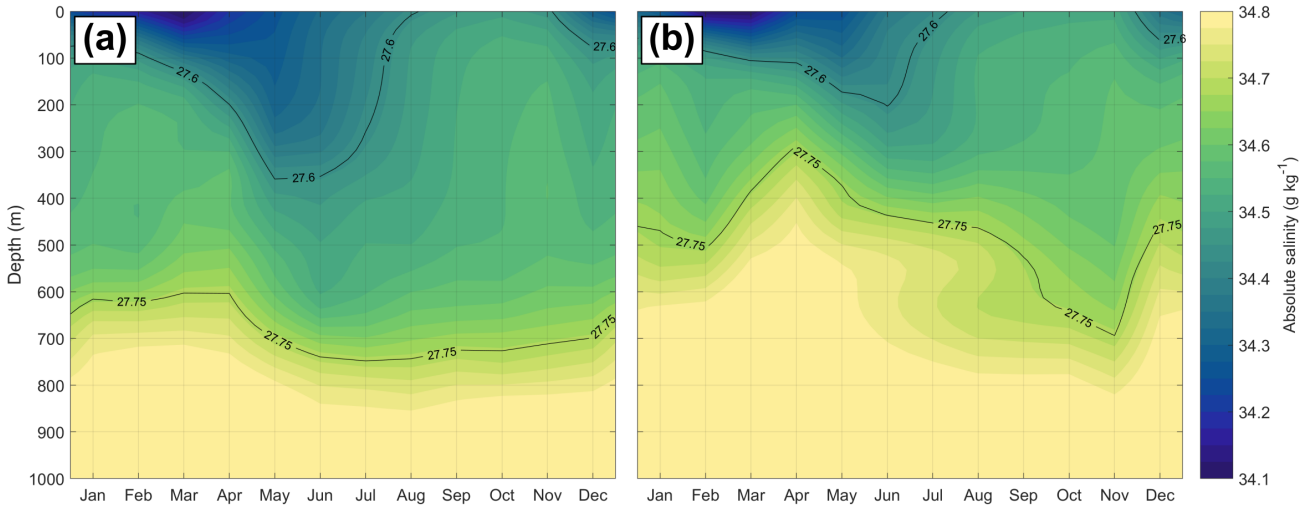

Figure S2. Time-depth Hovmöller diagrams of absolute salinity in the upper 1000 m of the H18 data over (a) $\mathrm{DML}_{\mathrm{shallow}}$ and (b) $\mathrm{DML}_{\mathrm{deep}}$ bathymetry. Contours show selected isolines of potential density in kg m^{-3}.

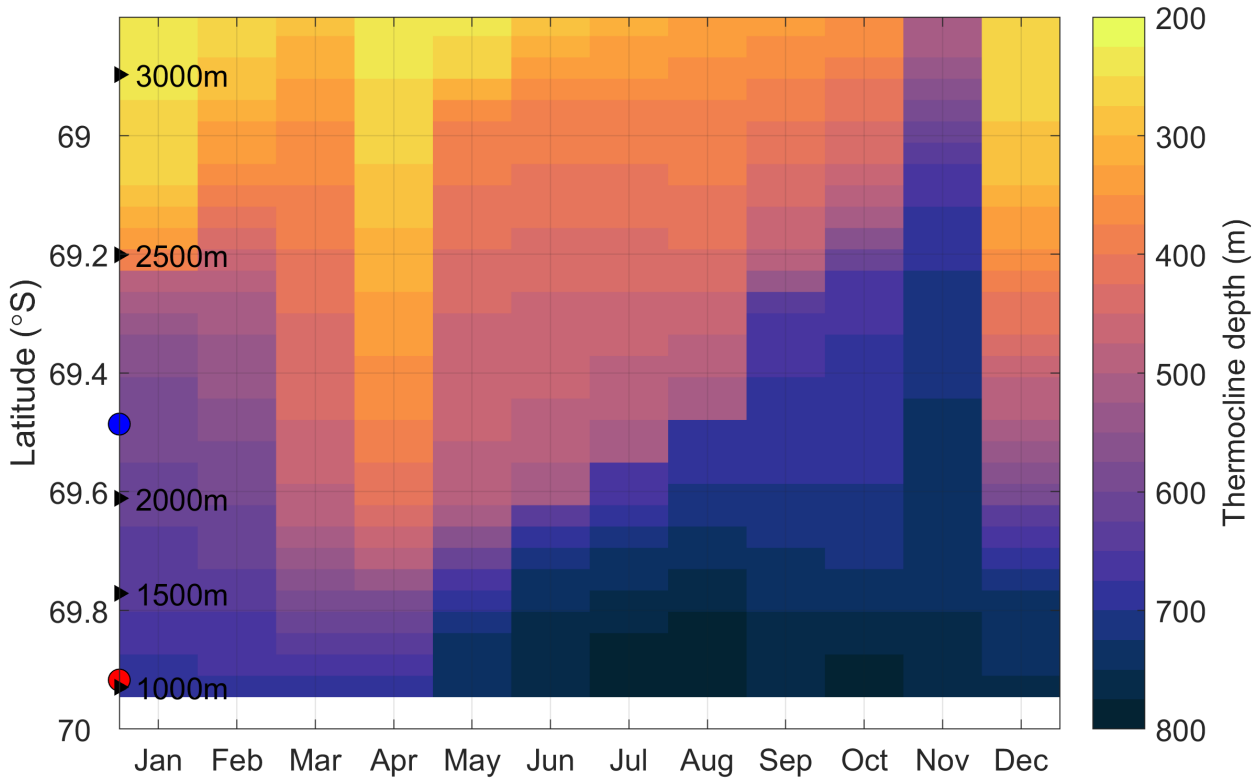

Figure S3. Time-latitude/bathymetry Hovmöller diagram of thermocline depth (−0.3 °C isotherm) of the H18 data projected on the bathymetry at 6°E. The grid and axis limits are the same as in Fig. 8a.

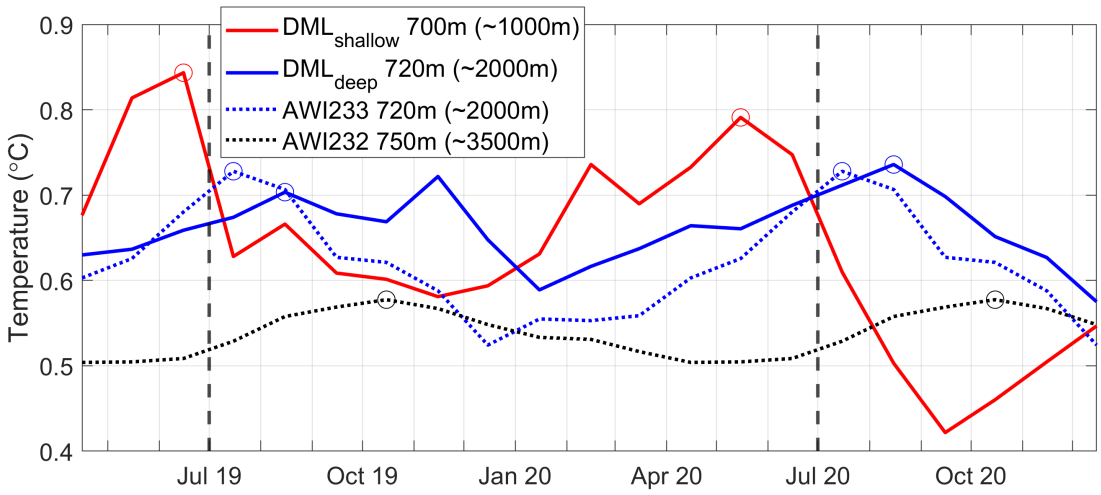

Figure S4. Comparison between temperatures at $DML_{shallow}$, DML_{deep}, AWI233 and AWI232 (both at the prime meridian). In the legend, the depth given after the mooring name is the rough depth for which the respective temperature is shown, and the depth in parentheses is the isobath over which the respective mooring is located. The circles indicate corresponding seasonal maxima between the different time series. For the AWI moorings, monthly mean climatologies are shown (AWI233: 1996-2008, AWI232: 1996-2016). The AWI-233 data are taken from Fahrbach and Rohardt (2012g), Fahrbach and Rohardt (2012h), Fahrbach and Rohardt (2012i), Fahrbach and Rohardt (2012j), Fahrbach and Rohardt (2012k), Fahrbach and Rohardt (2012l), Fahrbach and Rohardt (2012m), and Fahrbach and Rohardt (2012n). The AWI-232 data are taken from Fahrbach and Rohardt (2012a), Fahrbach and Rohardt (2012b), Fahrbach and Rohardt (2012c), Fahrbach and Rohardt (2012d), Fahrbach and Rohardt (2012e), Fahrbach and Rohardt (2012f), Fahrbach and Rohardt (2013a), Fahrbach and Rohardt (2013b), Fahrbach and Rohardt (2013c), Rohardt and Boebel (2017a), and Rohardt and Boebel (2015), Rohardt and Boebel (2017b).

$DML_{shallow}$ 69° 22.81' S, 10° 38.23' E / 1059 m		
Instrument	Depth	Duration
ADCP300	207 m	23.3.19 - 4.9.20
SBE37	213 m	23.3.19 - 29.12.20
SBE56	271 m	23.3.19 - 29.12.20
Aquadopp	332 m	23.3.19 - 29.12.20
SBE37	385 m	23.3.19 - 29.12.20
SBE56	447 m	23.3.19 - 29.12.20
SBE56	498 m	23.3.19 - 29.12.20
SBE56	550 m	23.3.19 - 29.12.20
SBE56	601 m	23.3.19 - 29.12.20
SBE56	652 m	23.3.19 - 29.12.20
SBE37	703 m	23.3.19 - 29.12.20
ADCP150	779 m	23.3.19 - 9.11.20
SBE56	814 m	23.3.19 - 29.12.20
SBE56	867 m	23.3.19 - 29.12.20
SBE56	920 m	23.3.19 - 29.12.20
SBE56	973 m	23.3.19 - 29.12.20
SBE37	1040 m	23.3.19 - 29.12.20
Aquadopp	1047 m	23.3.19 - 29.12.20

Table S1. Overview of instruments mounted on mooring $DML_{shallow}$. ADCP300 denotes a short-range 300 kHz ADCP, and ADCP150 a long-range 150 kHz ADCP. SBE 37 is a MicroCAT and SBE56 is a Thermistor.

DML_{deep} 69° 4.08' S, 6° 1.80' E / 2166 m		
Instrument	Depth	Duration
ADCP300	126 m	31.3.19 - 1.11.20
SBE37	132 m	26.3.19 - 5.1.21
SBE56	216 m	26.3.19 - 5.1.21
SBE56	269 m	26.3.19 - 5.1.21
SBE56	374 m	26.3.19 - 5.1.21
Aquadopp	451 m	31.3.19 - 5.1.21
SBE56	505 m	26.3.19 - 5.1.21
SBE56	558 m	26.3.19 - 5.1.21
SBE56	611 m	26.3.19 - 5.1.21
SBE56	663 m	26.3.19 - 5.1.21
SBE56	716 m	26.3.19 - 5.1.21
SBE56	769 m	26.3.19 - 5.1.21
SBE37	821 m	26.3.19 - 5.1.21
ADCP150	880 m	31.3.19 - 10.11.20
SBE56	923 m	26.3.19 - 5.1.21
SBE56	974 m	26.3.19 - 5.1.21
SBE37	2150 m	26.3.19 - 5.1.21
Aquadopp	2158 m	31.3.19 - 5.1.21

Table S2. Same as Table S1, but for DML_{deep}.